J|A|C|S
ARTICLES
Published on Web 11/13/2002

Enantioselective Formation of a Dynamic Hydrogen-Bonded Assembly Based on the Chiral Memory Concept

Tsutomu Ishi-i,[†,‡,§] Mercedes Crego-Calama,[†] Peter Timmerman,*[,†] David N. Reinhoudt,*[,†] and Seiji Shinkai[‡]

Contribution from the Laboratory of Supramolecular Chemistry and Technology, MESA+ Research Institute, University of Twente, P.O. Box 217, 7500 AE Enschede, The Netherlands and Chemotransfiguration Project, Japan Science and Technology Corporation (JST), 2432 Aikawa, Kurume, Fukuoka 839-0861, Japan

Received May 23, 2002

Abstract: In this paper, we report the enantioselective formation of a dynamic noncovalent double rosette assembly **1a**$_3$·(CYA)$_6$ composed of three 2-pyridylcalix[4]arene dimelamines (**1a**) and six butylcyanuric acid molecules (BuCYA). The six 2-pyridyl functionalities of the assembly interact stereoselectively with chiral dicarboxylic acids **3a**−**e** via two-point hydrogen-bonding interactions. One of the two enantiomeric assemblies (*P*- or *M*-) **1a**$_3$·(CYA)$_6$ is formed in excess as the result of the complexation of the chiral diacids, resulting in formation of optically active assemblies. The complexations with dibenzoly tartaric acids D-**3a** and L-**3a** (3 equivalent), respectively, leading to the formation of diastereomeric assemblies (*P*)-**1a**$_3$·(BuCYA)$_6$·(D-**3a**)$_3$ and (*M*)-**1a**$_3$·(BuCYA)$_6$·(L-**3a**)$_3$ with 90% diastereomeric excess. The diastereomeric excess in (*M*)-**1a**$_3$·(BuCYA)$_6$·(L-**3a**)$_3$ is "memorized" when L-**3a** is removed by precipitation with ethlylenediamine (EDA). The assembly (*M*)-**1a**$_3$·(BuCYA)$_6$ is still optically active (90% enantiomeric excess), although none of its individual components are chiral. (*M*)-**1a**$_3$·(BuCYA)$_6$ has a high kinetic stability toward racemization (E_a = 119 kJ mol^{-1}, half-life of (*M*)-**1a**$_3$·(BuCYA)$_6$ is ca. 1 week at 20 °C).

Introduction

Supramolecular chirality involves the nonsymmetrical arrangement of molecular components in noncovalent assemblies.[1,2] With the increased interest in noncovalent synthesis, control of supramolecular chirality has become an important issue. Most studies focus on assemblies that are a combination of achiral and chiral components, which can assemble either one or both of the two possible diastereoisomers.[3] Creation of enantiomerically pure assemblies is a lot more challenging. From a more philosophical point of view, amplification of one enantiomer in a dynamic noncovalent racemate may teach us valuable lessons on the origin of homochirality in nature.[4]

Two different methods for the chiral amplification of covalent systems can be found in the literature. The first method is based on covalent synthesis, in which a chiral source is introduced in macromolecular systems such as a polyisocyanate,[5,6] polystyrene−polyisocyanodipeptide,[7] polysilane,[8] polythiophene,[9] or a peptide nucleic acid.[10] Even small amounts of covalently incorporated chiral components govern the entire chiral structure of these macromolecules. This so-called Sergeants and Soldiers principle[5] results in chiral amplification to give species that have a much higher optical activity than expected from the chiral-to-achiral ratio. The created optically active macromolecule is regarded

* To whom correspondence should be addressed. E-mail: D.N.Reinhoudt@ct.utwente.nl; smct@ct.utwente.nl.
† University of Twente.
‡ Chemotransfiguration project, JST.
§ Present address: Institute of Advanced material Study, Kyushu University, 6−1 Kasuga-kohen, Kasuga 816-8580, Japan.

(1) Lehn, J.-M. *Supramolecular Chemistry, Concept and Perspectives*; VCH: Weinheim, 1995.
(2) (a) Suárez, M.; Branda, N.; Lehn, J.-M.; Decian, A.; Fischer, J. *Helv. Chim. Acta* **1998**, *81*, 1−13. (b) Geib, S. J.; Vicent, C.; Fan, E.; Hamilton, A. D. *Angew. Chem., Int. Ed. Engl.* **1993**, *32*, 119−121. (c) Seto C. T.; Whitesides, G. M. *J. Am. Chem. Soc.* **1993**, *115*, 905−916.
(3) For selected recent samples see: (a) Castellano, R. K.; Kim, B. H.; Rebek, J., Jr. *J. Am. Chem. Soc.* **1997**, *119*, 12671−12672. (b) Nuckolls, C.; Hof, F.; Martín, T.; Rebek, J., Jr. *J. Am. Chem. Soc.* **1999**, *121*, 10281−10285. (c) Castellano, R. K.; Nuckolls, C.; Rebek, J., Jr. *J. Am. Chem. Soc.* **1999**, *121*, 11156−11163. (d) Saito, S.; Nuckolls, C.; Rebek, J., Jr. *J. Am. Chem. Soc.* **2000**, *122*, 9628−9630. (e) Simanek, E. E.; Qiao, S.; Choi, I. S.; Whitesides, G. M. *J. Org. Chem.* **1997**, *62*, 2619−2621. (f) Russell, K. C.; Lehn, J.-M.; Kyritsakas, N.; DeCian, A.; Fischer, J. *N. J. Chem.* **1998**, 123−128. (g) Ghadiri, M. R.; Granja, J. R.; Milligan, R. A.; McRee, D. E.; Khazanovich, N. *Nature*, **1993**, *366*, 324−327. (h) Hanessian, S.; Gomtsyan, A.; Simard, M.; Roelens, S. *J. Am. Chem. Soc.*, **1994**, *116*, 4495−4496. (i) Fenniri, H.; Mathivanan, P.; Vidale, K. L.; Sherman, D. M.; Hallenga, K.; Wood, K. V.; Stowell, J. G. *J. Am. Chem. Soc.* **2001**, *123*, 3854−3855. (j) Rincón, A. M.; Prados, P.; de Mendoza, J. *J. Am. Chem. Soc.* **2001**, *123*, 3493−3498. (k) Ky Hirschberg, J. H. K.; Brunsveld, L.; Ramzi, A.; Vekemans, J. A. J. M.; Sijbesma, R. P.; Meijer, E. W. *Nature* **2000**, *407*, 167−170. (l) Schenning, A. P. H. J.; Jonkheijm, P.; Peeters, E.; Meijer, E. W. *J. Am. Chem. Soc.* **2001**, *123*, 409−416. (m) Kondo, T.; Oyama, K.; Yoshida, K. *Angew. Chem., Int. Ed.* **2001**, *40*, 894−897.
(4) (a) Bada, J. L. *Nature* **1995**, *347*, 594−595. (b) Cairns-Smith, A. G. *Chem. Br.* **1986**, 559−561. (c) Feringa, B. L.; van Delden, R. A. *Angew. Chem., Int. Ed.* **1999**, *38*, 3418−3438. (d) Soai, K.; Shibata, T.; Sato, I. *Acc. Chem. Res.* **2000**, *33*, 382−390.
(5) Green, M. M.; Reidy, M. P.; Johnson, R. J.; Darling, G.; O'Leary, D. J.; Willson, G. *J. Am. Chem. Soc.* **1989**, *111*, 6452−6454.
(6) Green, M. M.; Peterson, N. C.; Sato, T.; Teramoto, A.; Cook, R.; Lifson, S. *Science* **1995**, *268*, 1860−1866.
(7) Cornelissen, J. J. L. M.; Fischer, M.; Sommerdijk, N. A. J. M.; Nolte, R. J. M. *Science* **1998**, *280*, 1427−1430.
(8) Fujiki, M. *J. Am. Chem. Soc.* **1994**, *116*, 11976−11981.
(9) Langeveld-Voss, B. M. W.; Waterval, R. J. M.; Janssen, R. A. J.; Weijer, E. W. *Macromolecules* **1999**, *32*, 227−230.
(10) Kozlov, I. A.; Orgel, L. E.; Nielsen, P. E. *Angew. Chem., Int. Ed.* **2000**, *39*, 4292−4295.

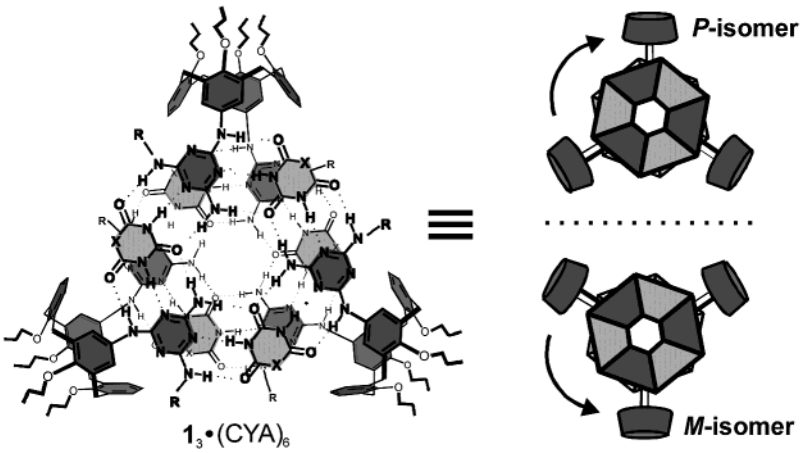

Figure 1. *P*- and *M*-isomers for D_3 symmetrical rosette assemblies.

as a diastereoisomer, although it contains only a tiny amount of the chiral source. The second method is based on the chiral memory concept in noncovalent synthesis, from which enantiomerically pure covalent systems are created (e.g., cis−transoidal polyacetylene,[11] saddle-shaped porphyrin,[12] cerium(IV) double decker porphyrin,[13] and zinc (II) porphyrin dimer[14]). In these memory systems, first a chiral auxiliary, used as additive, interacts stereoselectively in a noncovalent manner to give preferentially one of the two possible enantiomeric forms. Then, the additive is removed or replaced by an achiral additive to preserve the induced chirality.[11−14] The resulting enantiomer is still optically active, although none of its components are chiral.

We[15] and others[16] have reported chiral amplification via the Sergeants and Soldiers principle in noncovalent systems, resulting in highly ordered diastereomeric assemblies. However, to the best of our knowledge, chiral amplification combined with the chiral memory concept for the formation of enantiomeric assemblies has never been previously reported. Moreover, chiral memory is rare in nocovalent supramolecular assemblies,[17] because the additives that induce or preserve the supramolecular chirality often interfere with the noncovalent interactions that hold the assembly together.[18,19] Rebek et al. have reported a nice example of an enantioselective synthesis of a hydrogen-bonded dimeric capsule by inclusion of a suitable chiral guest molecule.[20] The induced supramolecular chirality is preserved when the chiral guest is replaced by an achiral one. The enantioselectivity is modest (50% ee) and the lifetime is limited ($t_{1/2}$, ca. 10−20 h).

We have been extensively studying hydrogen-bonded assemblies of type $\mathbf{1}_3\cdot(\mathrm{CYA})_6$ composed of nine different components, that is, three calix[4]arene dimelamines **1** and six cyanuric acid (CYA) derivatives (Figure 1).[21] A total of 36 cooperative hydrogen bonds hold the components together forming a double rosette. In this type of assembly, 3 isomeric forms (D_3, C_s, and C_{3h}) are possible, from which the chiral D_3-isomer is predominantly formed.[22] In the absence of chiral components in the assembly, the D_3-isomer exists as a racemic mixture of the *P*- and *M*-enantiomers (Figure 1). However, chiral centers introduced in either **1** or CYA fully induce chirality in the assembly and only one of the two diastereoisomers is formed.[23] More interestingly, when the chiral components are replaced by achiral ones, enantiomerically pure assemblies are obtained. These enantiomeric assemblies have high kinetic stability toward racemization with long lifetimes of ca. 3−4 days.[24] In these systems, the enantiomerically pure assemblies are obtained from the corresponding pure diastereoisomers and not by resolution of the enantiomeric racemic mixture.

In this paper, we report the enantioselective formation of chiral double rosette assemblies from a racemic dynamic mixture of *P*- and *M*-enantiomers. Six amino functionalities positioned on the assembly interact with chiral carboxylic acid auxiliaries via amine−carboxylic acid interaction to diastereoselectively form a *P*- or *M*-assembly.[25] Subsequently, the chiral acids are removed by complexation with an added amine and the

(11) Yashima, E.; Maeda, K.; Okamoto, Y. *Nature* **1999**, *399*, 449−451.
(12) Furusho, Y.; Kimura, T.; Mizuno, Y.; Aida, T. *J. Am. Chem. Soc*. **1997**, *119*, 5267−5268.
(13) Sugasaki, A.; Ikeda, M.; Takeuchi, M.; Robertson, A.; Shinkai, S. *J. Chem. Soc., Perkin Trans. 1* **1999**, 3259−3264.
(14) Kubo, Y.; Ohno, T.; Yamanaka, J.; Tokita, S.; Iida, T.; Ishimaru, Y. *J. Am. Chem. Soc*. **2001**, *123*, 12700−12701.
(15) Prins, L. J.; Timmerman, T.; Reinhoudt, D. N. *J. Am. Chem. Soc*. **2001**, *123*, 10153−10163.
(16) (a) Palmans, A. R. A.; Vekemans, J. A. J. M.; Havinga, E. E.; Meijer, E. W. *Angew. Chem., Int. Ed. Engl.,* **1997**, *36*, 2648−2651. (b) Brunsveld, L.; Lohmeijer, B. G. G.; Vekemans, J. A. J. A.; Meijer, E. W. *Chem. Commun*. **2000**, 2305−2306. (c) Brunsveld, L.; Schenning, A. P. H. J.; Broeren, M. A. C.; Janssen, H. M.; Vekemans, J. A. J. M.; Meijer, E. W. *Chem. Lett.* **2000**, 292−293.
(17) For chiral inductions at the supramolecular level by chiral additives see: (a) Rivera, J. M.; Martín, T.; Rebek, J., Jr. *Science* **1998**, *279*, 1021−1023. (b) Rivera, J. M.; Martín, T.; Rebek, J., Jr. *J. Am. Chem. Soc*. **2001**, *123*, 5213−5220. (c) Hiraoka, S.; Fujita, M. *J. Am. Chem. Soc*. **1999**, *121*, 10239−10240. (d) Ikeda, A.; Udzu, H.; Zhong, Z.; Shinkai, S.; Sakamoto, S.; Yamaguchi, K. *J. Am. Chem. Soc*. **2001**, *123*, 3872−3877.
(18) For reviews of hydrogen-bonded assemblies see: (a) Conn, M. M.; Rebek, J., Jr. *Chem. Rev*. **1997**, *97*, 1647−1668. (b) Rebek, J., Jr. *Acc. Chem. Res*. **1999**, *32*, 278−286. (c) Rebek, J., Jr. *Chem. Commun*. **2000**, 637−643. (d) Prins, L. J.; Timmerman, P.; Reinhoudt, D. N. *Angew. Chem., Int. Ed*. **2001**, *40*, 2382−2426.
(19) For reviews of metal-coordinative assemblies see: (a) Linton, B.; Hamilton, A. D. *Chem. Rev*. **1997**, *97*, 1669−1680. (b) Stang, P. J.; Olenyuk, B. *Acc. Chem. Res*. **1997**, *30*, 502−518. (c) Fujita, M. *Chem. Soc. Rev*. **1998**, *27*, 417−425. (d) Caulder, D. L.; Raymond, K. N. *Acc. Chem. Res*. **1999**, *32*, 975−982. (e) Caulder, D. L.; Raymond, K. N. *J. Chem. Soc., Dalton Trans*. **1999**, 1185−1200. (f) Leininger, S.; Olenyuk, B.; Stang, P. J. *Chem. Rev*. **2000**, *100*, 853−907. (g) Fujita, M.; Umemoto, K.; Yoshizawa, M.; Fujita, N.; Kusukawa, T.; Biradha, K. *Chem. Commun*. **2001**, 509−519.
(20) Rivera, J. M.; Craig, S. L.; Martín, T.; Rebek, J., Jr. *Angew. Chem., Int. Ed*. **2000**, *39*, 2130−2132.
(21) Timmerman, P.; Vreekamp, R. H.; Hulst, R.; Verboom, W.; Reinhoudt, D. N.; Rissanen, K.; Udachin, K. A.; Ripmeester, J. *Chem. Eur. J*. **1997**, *3*, 1823−1832.
(22) Prins, L. J.; Jolliffe, K. A.; Hulst, R.; Timmerman, P.; Reinhoudt, D. N. *J. Am. Chem. Soc*. **2000**, *122*, 3617−3627.
(23) Prins, L. J.; Huskens, J.; de Jong, F.; Timmerman, P.; Reinhoudt, D. N. *Nature* **1999**, *398*, 498−502.
(24) Prins, L. J.; de Jong, F.; Timmerman, P.; Reinhoudt, D. N. *Nature* **2000**, *408*, 181−184.
(25) Ishi-i, T.; Crego-Calama, M.; Timmerman, P.; Reinhoudt, D. N.; Shinkai, S. *Angew. Chem., Int. Ed*. **2002**, *41*, 1924−1929.

Chart 1

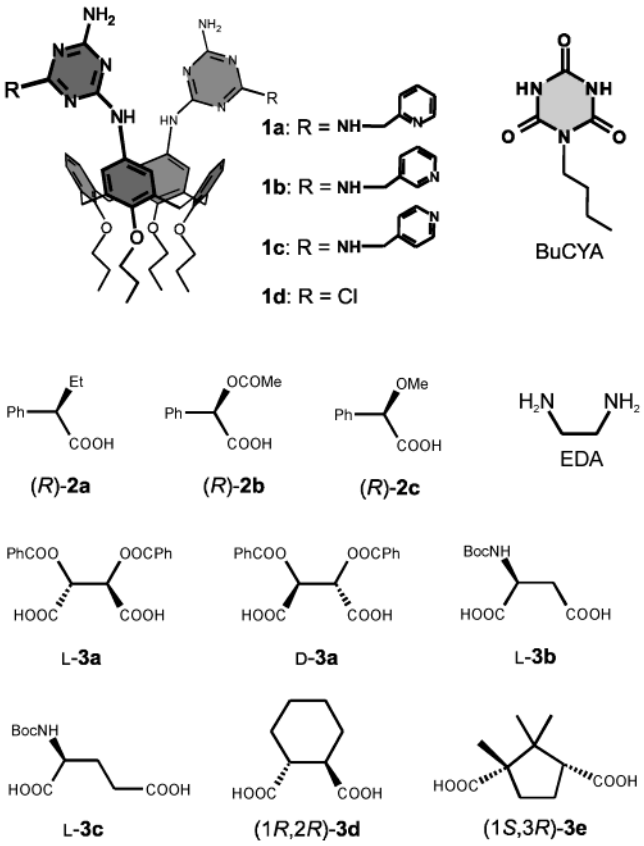

enantiomeric assembly (*P*- or *M*-) is obtained. These enantiomeric assemblies (90% ee in the best case) have a very long lifetime ($t_{1/2}$, ca. 1 week).

Results and Discussion

Preparation. Calix[4]arene-dimelamines **1a**−**c** with two pendant pyridyl groups were prepared from bis(chlorotriazine) **1d** by treatment with the corresponding aminomethylpyridines, that is, 2-aminomethylpyridine, 3-aminomethylpyridine, and 4-aminomethylpyridine, at 90 °C (Chart 1). The pyridyl groups are introduced in the double rosette assembly **1a**−**c**$_3$·(BuCYA)$_6$ as binding sites for chiral carboxylic acids.

Chiral Induction in 2-Pyridyl Assembly System 1a$_3$·(BuCYA)$_6$. We studied the complexation of double rosette assemblies **1a**$_3$·(BuCYA)$_6$ with a variety of chiral dicarboxylic acids **3**. Typically, 3 equiv of **3** were added to a solution of **1a**$_3$·(BuCYA)$_6$ (1.0 mM) in toluene-d_8 at 20 °C (ratio of COOH/pyridine = 1/1) and the mixtures were equilibrated over 15 h. The interaction between the assembly and the chiral diacid becomes apparent from shifts and splitting of signals in the ^{1}H NMR spectra. For example, in L-**3a** (3 equiv) the signals H^a, H^b, H^c, H^h, and H^i protons are split and shifted because of the formation of the diastereomeric assemblies (*M*)-**1a**$_3$·(BuCYA)$_6$·(L-**3a**)$_n$ and (*P*)-**1a**$_3$·(BuCYA)$_6$·(L-**3a**)$_n$. These are no longer mirror images and exhibit different signals in the ^{1}H NMR spectrum (Figure 2).[23]

The ratio of these signals shows that most diacids **3a**−**e** bind preferentially to either the *M*- or the *P*-enantiomer of assembly **1a**$_3$·(BuCYA)$_6$. This leads to amplification of that particular enantiomer in the mixture, as both enantiomers are in dynamic equilibrium. Diastereomeric excess (de) is estimated from the integration ratio of the split NMR signals of either H^a, H^c, or H^h (Figure 2). The addition of dicarboxylic acids **3a**−**e** (3 equiv) gives a very high enantioselectivity. The highest selectivity was achieved with **3a** (90% de, runs 4 and 5 in Table 1). The high de values found for dicarboxylic acids are ascribed to two-point hydrogen-bonding interaction between one molecule of **3** and the two 2-pyridine moieties of **1a**$_3$·(BuCYA)$_6$.[26] In contrast, when monocarboxylic acids **2a**−**c** (6 equiv, ratio of COOH/pyridine = 1/1) were added, only 0−10% de were obtained (runs 1−3 in Table 1). In this case, the 2-pyridyl moiety in **1a**$_3$·(BuCYA)$_6$ probably forms a complex with **2a**−**c** only by a one-point interaction.

Table 1. Induction of Chirality in Assembly **1a**$_3$·(BuCYA)$_6$ as a Result of the Addition of Chiral Acids **2a**−**c** and **3a**−**e**[a]

run	**2** or **3**	de (%)[b]	helicity[d]	CD$_{306}$ (mdeg)[e]
1	(*R*)-**2a**	0		0
2	(*R*)-**2b**	8−10[c]	M	5.6
3	(*R*)-**2c**	0		0
4	L-**3a**	90	M	53.0
5	D-**3a**	90	P	−52.3
6	L-**3b**	36	M	18.8
7	L-**3c**	30	M	18.0
8	(1*R*,2*R*)-**3d**	17	M	9.8
9	(1*S*,3*R*)-**3e**	5−6[c]	M	3.3

[a] Conditions: toluene-d_8, [**1a**$_3$·(BuCYA)$_6$] = 1.0 mM, [**2**]/[**1a**$_3$·(BuCYA)$_6$] = 6/1, [**3**]/[**1a**$_3$·(BuCYA)$_6$] = 3/1, at 20 °C. Under these conditions the assemblies were quantitatively formed as a single D_3-isomer. [b] Determined by integration of the ^{1}H NMR signals H^{a1} and H^{a2}. [c] Calculated from the CD intensity at 306 nm (for details, see supporting data). [d] Helicity of the preferentially formed isomer (*M*- or *P*-) of assembly **1a**$_3$·(BuCYA)$_6$, assigned on the basis of the CD sign. [e] CD intensity (mdeg) at 306 nm.

In the absence of the chiral auxiliary, the racemic mixture of *P*- and *M*-enantiomers is not CD-active. When the chiral acids are added, the CD spectra of **1a**$_3$·(BuCYA)$_6$ show reproducible Cotton effects (Figure 3). This indicates that the chiral acids interact with assembly **1a**$_3$·(BuCYA)$_6$, thus enforcing an excess of either the *P*- or the *M*-enantiomer in the mixture. Generally, we found that chiral L-acids induce *M*-helicity, as indicated from a positive CD sign.[23] Similarly, *P*-helicity is induced by D-acids. The CD spectra for the complexes (*M*)-**1a**$_3$·(BuCYA)$_6$·(L-**3a**)$_3$ and (*P*)-**1a**$_3$·(BuCYA)$_6$·(D-**3a**)$_3$ are almost perfect mirror images (Figure 3).

There are two possible modes of complexation that could account for the two-point interactions found in the dicarboxylic acid-complexations, that is, sideways (diacid interacting with both floors of the double rosette) or on top (or bottom) positions of **1a**$_3$·(BuCYA)$_6$, (for the side complexation see Figure 4). CPK models indicate that only the sideways complexation is possible, because in the top (or bottom) complexation the distance between the 2-pyridyl groups on the same rosette floor is too large to interact with **3** in a two-point fashion. The distance between two neighboring pyridyl groups on different rosette floors is smaller (Figure 4). Such a chiral arrangement is very suitable for the complexation with L-**3a**, in which the two carboxyl groups are preorganized in a trans-configuration.[27]

Influence of Pyridine Moiety in Assemblies. The observed selectivity for complexation of chiral diacids **3** is very sensitive to structural changes in the pyridyl functionalities. In contrast

(26) (a) Takeuchi, M.; Imada, T.; Shinkai, S. *Angew. Chem., Int. Ed.* **1998**, *37*, 2096−2099. (b) Ikeda, M.; Takeuchi, M.; Sugasaki, A.; Robertson, A.; Imada, T.; Shinkai, S. *Supramol. Chem.* **2000**, *12*, 321−345.
(27) Garcia-Tellado, F.; Albert, J.; Hamilton, A. D. *J. Chem. Soc., Chem. Commun.* **1991**, 1761−1763.

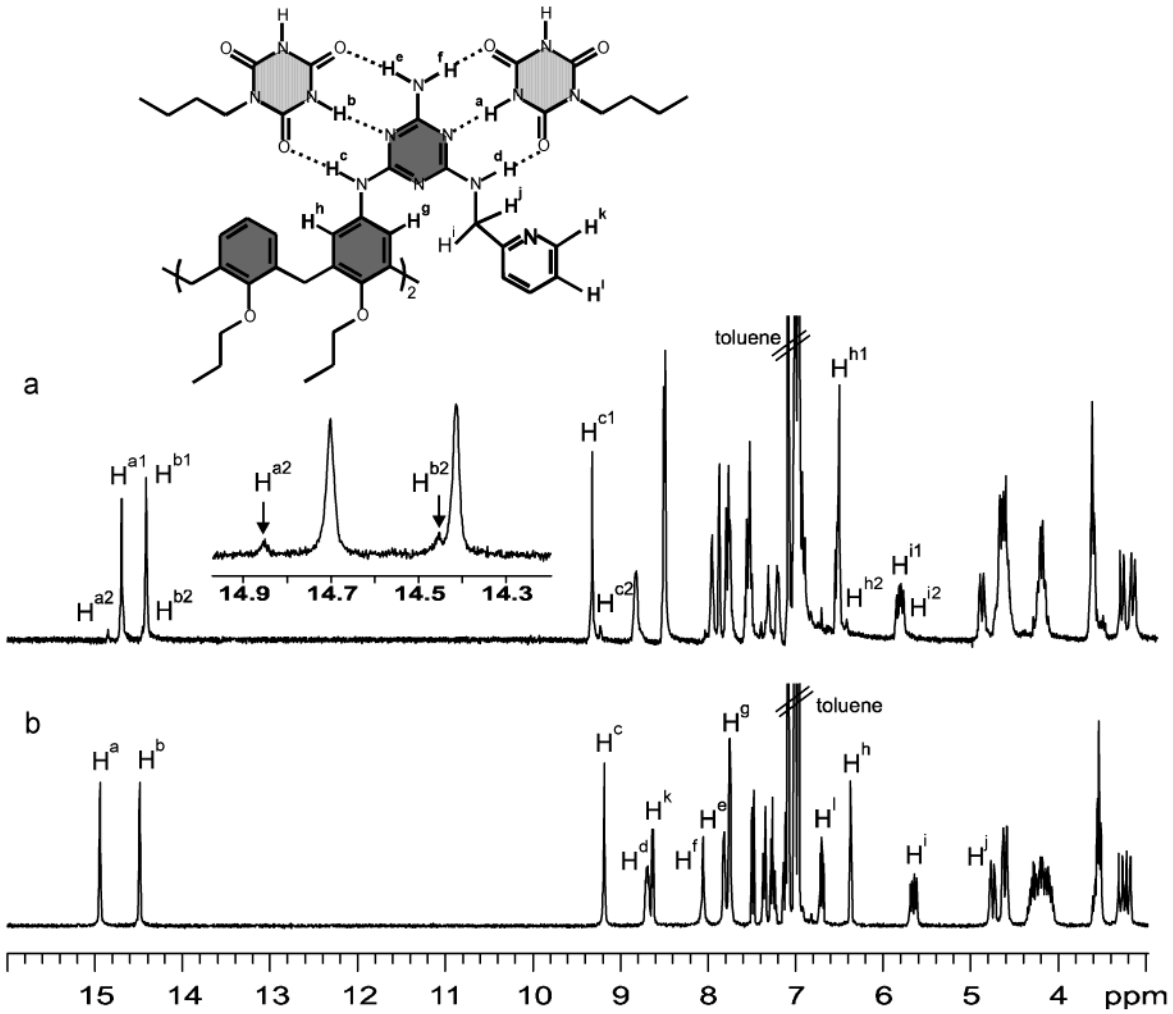

Figure 2. ^{1}H NMR spectra of **1a**$_3$·(BuCYA)$_6$ (1 mM) in toluene-d_8 at 20 °C in the presence of (a) 3 equiv and (b) 0 of L-**3a**.

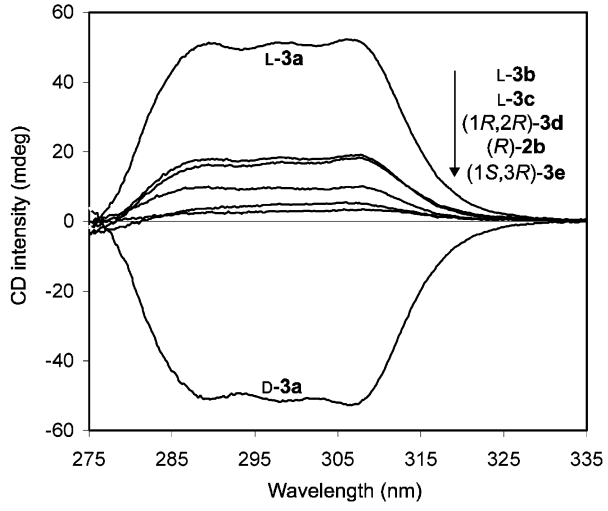

Figure 3. CD spectra of **1a**$_3$·(BuCYA)$_6$ (1 mM) in toluene-d_8 in the presence of (*R*)-**2b** (6 equiv), L-**3a**, D-**3a**, L-**3b**, L-**3c**, (1*R*,2*R*)-**3d**, (1*S*,3*R*)-**3e** (3 equiv) (in 0.01-cm width cell at 20 °C).

to assembly **1a**$_3$·(BuCYA)$_6$ with a 2-pyridyl group, **1b**$_3$·(BuCYA)$_6$ and **1c**$_3$·(BuCYA)$_6$ with a 3-pyridyl and 4-pyridyl groups, respectively, are formed as mixtures of D_3-, C_{3h}-, and C_s-symmetrical isomers.[22] Upon the addition of **3**, the ratio of the three isomers changed and the population of D_3-isomer increased (Tables 2 and 3).[28] Upon the addition of **3a**−**d** to

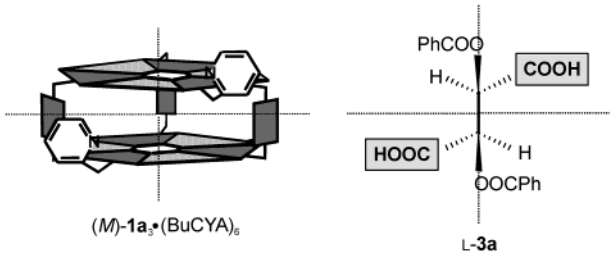

Figure 4. Chiral arrangement of the binding sites for the complexation of (*M*)-**1a**$_3$·(BuCYA)$_6$ with L-**3a**.

1b$_3$·(BuCYA)$_6$ and **1c**$_3$·(BuCYA)$_6$, in the CD spectra Cotton effects were also observed, but judging from the CD intensity at 306 nm, a high chiral induction could not be achieved (Tables 2 and 3). **1c**$_3$·(BuCYA)$_6$ formed gel and gel-like viscous solutions with **3a**−**c** (Table 3).[29] These results indicate that only the 2-pyridyl functionality is suitable for complexation with the chiral dicarboxylic acid and to induce a preference for the *P*- or *M*-enantiomer in the racemic mixture.

(28) The change of the isomer ratio could be ascribed to the polarity change of medium by the additions of polar additives **3** because generally population of D_3-isomer tends to increase with increasing solvent polarity.

(29) The one-dimensional aggregates formed in the gel samples may be ascribed to intermolecular pyridine−carboxylic acid interactions. For reviews of low-molecular-weight organogels see: (a) van Esch, J.; Schoonbeek, F.; de Loose, M.; Veen, E. M.; Kellogg, R. M.; Feringa, B. L. *Supramol. Sci.* **1999**, *6*, 233−259. (b) Shinkai, S.; Murata, K. *J. Mater. Chem.* **1998**, *8*, 485−495. (c) Terech, P.; Weiss, R. G. *Chem. Rev.* **1997**, *97*, 3133−3159.

Table 2. Induction of Chirality in Assembly $\mathbf{1b}_3$·(BuCYA)$_6$ as a Result of the Addition of Chiral Acids **3a**−**e**[a]

run	**3**	$D_3/C_{3h}/C_s$[b]	helicity[c]	CD_{306} (mdeg)[d]
1		78:10:12		
2	L-**3a**	80:12:8		*e*
3	L-**3b**	89:5:6	M	8.0
4	L-**3c**	73:15:12	P	−1.5
5	(1*R*,2*R*)-**3d**	81:9:10	M	12.9
6	(1*S*,3*R*)-**3e**	83:9:8		0

[a] Conditions: toluene-d_8, [$\mathbf{1b}_3$·(BuCYA)$_6$] = 1.0 mM, [**3**]/[$\mathbf{1b}_3$·(BuCYA)$_6$] = 3/1, at 20 °C. Under these conditions the assemblies were quantitatively formed as a mixture of D_3-, C_{3h}-, and C_s-isomers. [b] Molar ratio of D_3-, C_{3h}-, and C_s-isomers determined by integration of the ^{1}H NMR signals H^a and H^b. [c] Helicity of the preferentially formed isomer (*M*- or *P*-) of assembly $\mathbf{1b}_3$·(BuCYA)$_6$, assigned on the basis of the CD sign. [d] CD intensity (mdeg) at 306 nm. [e] Could not be determined because of precipitation.

Table 3. Induction of Chirality in Assembly $\mathbf{1c}_3$·(BuCYA)$_6$ as a Result of the Addition of Chiral Acids **3a**−**e**[a]

run	**3**	yield (%)[b]	$D_3/C_{3h}/C_s$[f]	helicity[g]	CD_{306} (mdeg)[i]
1		90	20:20:60		
2	L-**3a**	0[c]		h	−12.3[j]
3	L-**3b**	20[d]		P	−1.1
4	L-**3c**	40[d]			0
5	(1*R*,2*R*)-**3d**	80	83:4:13	P	−0.8
6	(1*S*,3*R*)-**3e**	*e*			

[a] Conditions: toluene-d_8, [$\mathbf{1c}_3$·(BuCYA)$_6$] = 1.0 mM, [**3**]/[$\mathbf{1c}_3$·(BuCYA)$_6$] = 3/1, at 20 °C. [b] The assembly formation was determined by integration of the $ArCH_2Ar$ and the NH/ArH^h proton signals in the ^{1}H NMR spectrum. [c] Gel. [d] Gel-like viscous solution. [e] Precipitate. [f] Molar ratio of D_3-, C_{3h}-, and C_s-isomers determined by integration of the ^{1}H NMR signals H^a and H^b. [g] Helicity of the preferentially formed isomer (*M*- or *P*-) of assembly $\mathbf{1c}_3$·(BuCYA)$_6$, assigned on the basis of the CD sign. [h] The different CD pattern was observed. [i] CD intensity (mdeg) at 306 nm. [j] CD intensity (mdeg) at 312 nm.

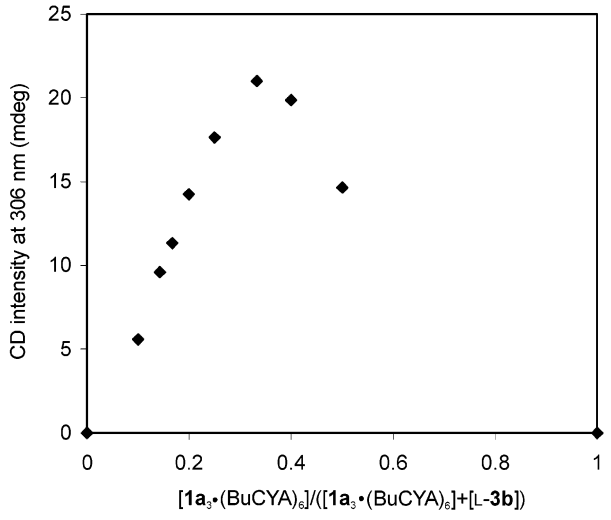

Figure 5. Job plot for the complexation of $\mathbf{1a}_3$·(BuCYA)$_6$ with L-**3b**: the sum of [$\mathbf{1a}_3$·(BuCYA)$_6$] and [L-**3b**] was maintained constant (4 mM in toluene).

Stoichiometry of the Complexes of Double Rosette Assemblies with Diacids. The stoichiometry of the complexes of $\mathbf{1a}_3$·(BuCYA)$_6$ with **3** was determined by a Job plot analysis (Figure 5).[30] The plot of the CD intensity at 306 nm versus the ratio of [$\mathbf{1a}_3$·(BuCYA)$_6$]/([$\mathbf{1a}_3$·(BuCYA)$_6$]+[L-**3b**]) exhibits a clear maximum at 0.33, suggesting the formation of 1:2 complex $\mathbf{1a}_3$·(BuCYA)$_6$·(L-**3b**)$_2$ as the main species (Scheme 1).[31]

(30) Job, A. *Ann. Chim.* **1928**, *9*, 113−134.
(31) Reliable results could not be obtained from a Job plot for the complexation with L-**3a** because of solubility problems.

Scheme 1. Schematic Representation of the Cooperative Interaction of $\mathbf{1a}_3$·(BuCYA)$_6$ with L-**3**

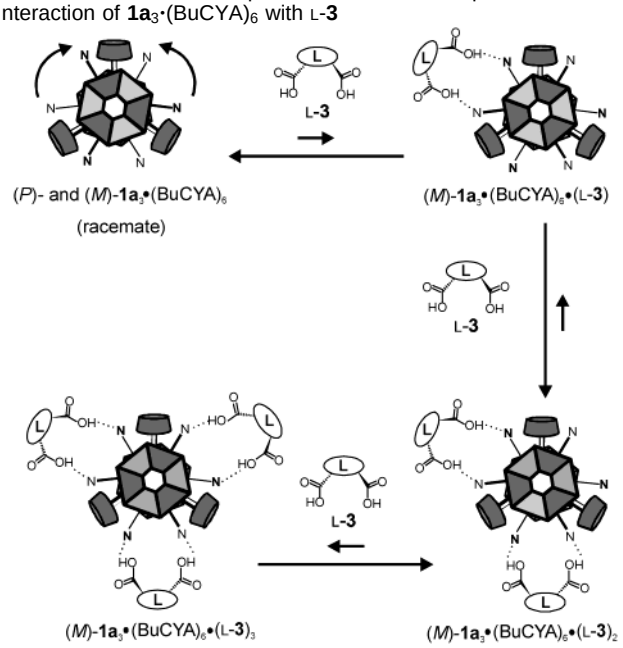

More valuable information about the structure of the complex of $\mathbf{1a}_3$·(BuCYA)$_6$ with **3** was obtained from CD titration studies. The CD intensity at 306 nm increases nonlinearly upon addition of L-**3a** or L-**3b** (Figure 6). Interestingly, both the two CD titrations display sigmoidal curvatures, which is a sign of homotropic positive allosterism arising from cooperativity in the complexation process (Figure 6).[32] The cooperativity was analyzed using the Hill eq 1,[33] where [*G*] is the concentration of guest (L-**3a** or L-**3b**), *K* is the association constant, *n* is the Hill coefficient, CD_{obs} is the observed CD intensity, and CD_{sat} is the saturated CD intensity.[34]

$$y = K/([G]^{-n} + K) = CD_{obs}/CD_{sat}$$

$$\log(y/(1-y)) = n\log[G] + \log K \qquad (1)$$

From a plot of $\log(y/(1-y))$ against $\log[G]$, values of $\log K = 5.64$ and $n = 1.96$ were calculated for L-**3a** (correlation coefficient, 0.997). For L-**3b**, values of $\log K = 5.38$ and $n = 1.82$ (correlation coefficient, 0.999) were obtained (for details see supporting data). Generally, *n* expresses not only the degree of cooperativity but also the number of binding sites. Thus, these *n* values 1.82−1.96 agree well with the result of the Job plot, which indicate that the main species is the 1:2 complex $\mathbf{1a}_3$·(BuCYA)$_6$·(L-**3**)$_2$. The observed positive allosterism was also analyzed by Scatchard plots,[35] in which Hill coefficients (*n*)

(32) Shinkai, S.; Ikeda, M.; Sugasaki, A.; Takeuchi, M. *Acc. Chem. Res.* **2001**, *34*, 494−503.
(33) Connors, K. A. *Binding Constants*; Wiley: New York, 1987.
(34) In the titrations, we could not directly estimate the saturated CD intensity, because upon the addition of >2.4 equiv of L-**3a**, trace amounts of precipitates were formed making it difficult to obtain reliable CD values. Further, upon addition of >2.7 equiv of L-**3b**, the CD intensity slightly decreased because of the dissociation of the assembly (Figure 6). Therefore, the CD intensities at 306 nm were corrected on the basis of the linear plots with the de values (correlation coefficients, 0.997 for L-**3a** and 0.998 for L-**3b**, see supporting data), from which the saturated CD intensities can be estimated as ∼65.1 mdeg for L-**3a** and 21.8 mdeg for L-**3b** (see supporting data). For the linear plots, we assumed that the magnitude of the induced CD for the three CD-active species (1:1, 1:2, and 1:3 complexes) is roughly the same (for details see ref 17). Thus, the calculated CD intensities include large error. The solubility problem could not be improved using *n*-octadecyl-CYA bearing a more soluble functionality.
(35) Permutter-Hayman, B. *Acc. Chem. Res.* **1986**, *19*, 90−96.

Scheme 2. Formation of the Enantiomeric Assembly (*M*)-**1a**$_3$·(BuCYA)$_6$ and Its Racemization

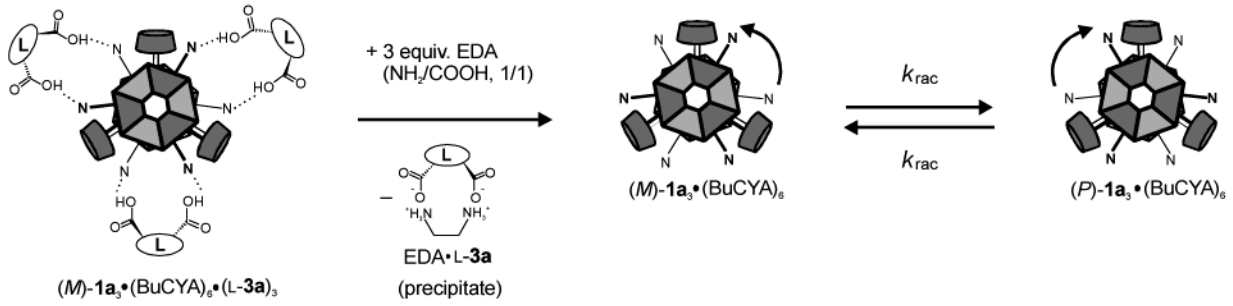

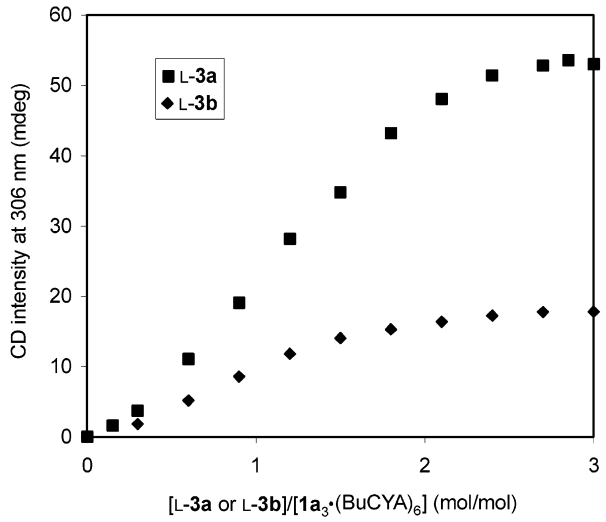

Figure 6. Plots of CD values (mdeg) at 306 nm versus [L-**3a** or L-**3b**]/[**1a**$_3$·(BuCYA)$_6$] for the titrations of **1a**$_3$·(BuCYA)$_6$ by L-**3a** and L-**3b**: in toluene-d_8, [**1a**$_3$·(BuCYA)$_6$] = 1 mM, at 20 °C.

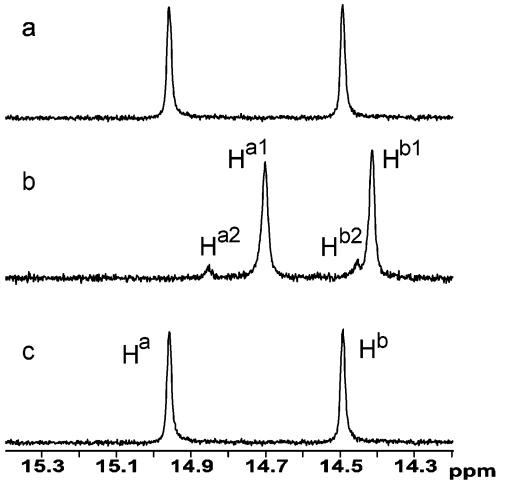

Figure 7. ^{1}H NMR titration of **1a**$_3$·(BuCYA)$_6$ (1 mM) with L-**3a** and EDA in toluene-d_8 at 20 °C: (a) with 3 equiv of L-**3a** and subsequently with 3 equiv of EDA, (b) with 3 equiv of L-**3a**, (c) without L-**3a** and EDA.

are correlated with the maximum values (y_{max}) according to a equation of $n = 1/(1 - y_{max})$. The positive or negative allosterism is expressed by the upward and downward curvature, respectively. From the plots of y versus y/[L-**3a** or L-**3b**], we have obtained values of y_{max} around 0.5 ($n = 2.0$) with upward curvatures (see supporting data). The plots are rather flat, indicating that the cooperativity is not so high. This means that also 1:1 and 1:3 complexes **1a**$_3$·(BuCYA)$_6$·(L-**3**) and **1a**$_3$·(BuCYA)$_6$·(L-**3**)$_3$ will be present as minor species (Scheme 1). The formation of a 1:2 complex as the main species might be attributed to either simple steric effects or allosteric conformational changes,[32] but the details are not yet clear.

Memory of Induced Supramolecular Chirality. The induced supramolecular *M*-chirality in the diastereomeric assembly (*M*)-**1a**$_3$·(BuCYA)$_6$·(L-**3a**)$_3$ is preserved when the L-**3a** moieties are removed by complexation with ethylenediamine (EDA), leading to formation of mainly the *M*-enantiomer of **1a**$_3$·(BuCYA)$_6$ (Scheme 2).

The removal of L-**3a** from (*M*)-**1a**$_3$·(BuCYA)$_6$·(L-**3a**)$_3$ can be monitored by ^{1}H NMR spectroscopy. After the addition of L-**3a** (3 equiv) to the racemic mixture **1a**$_3$·(BuCYA)$_6$ (>15 h), each singlet signal H^a and H^b is shifted upfield and split to a pair of singlets (Figure 7c,b). By the subsequent addition of 3 equiv of EDA, within a few minutes the initial resonances were regenerated, indicating the complete removal of L-**3a** (Figure 7a). Under these present conditions, no resonances corresponding to EDA and L-**3a** species are observed in the ^{1}H NMR spectrum. The removal of L-**3a** is also easily visible, because a precipitate is formed which was identified by ^{1}H NMR spectroscopy and elemental analysis as the EDA·L-**3a** 1:1 complex.[36] Thus, by using stoichiometric amounts of EDA (3 equiv) the chiral auxiliary L-**3a** is completely removed as a precipitate and only assembly **1a**$_3$·(BuCYA)$_6$ is present in solution predominately as an enantiomer with the *M*-chirality. The induced chirality is memorized by the assembly, and (*M*)-**1a**$_3$·(BuCYA)$_6$ is obtained with an optical purity of 90% ee (enantiomeric excess).

The preservation of the optical purity of (*M*)-**1a**$_3$·(BuCYA)$_6$ is corroborated by means of ^{1}H NMR titration studies. The integration ratio of the two H^{a1} and H^{a2} peaks (see Figure 7b), which correspond to *M* and *P* isomers, respectively, was not changed when 0, 0.6, 1.2, and 1.8 equiv of EDA were added to (*M*)-**1a**$_3$·(BuCYA)$_6$·(L-**3a**)$_3$. Further evidence was obtained from CD spectroscopy. After the addition of EDA to (*M*)-**1a**$_3$·(BuCYA)$_6$·(L-**3a**)$_3$, at 20 °C the assembly was still CD-active even in the absence of any chiral sources. The magnitude of the CD signal was of the same order before and after the addition of EDA (Figure 8). The slow racemization rate of (*M*)-**1a**$_3$·(BuCYA)$_6$ is also in line with the preservation of 90% ee, as described below in detail.[37]

(36) ^{1}H NMR analysis (CD_3OD) of the precipitate indicated the 1:1 ratio of EDA: L-**3a**. The C*H*N and C*H*COO signals in EDA·L-**3a** shifted downfield (δ 3.17 ppm, $\Delta\delta$ +0.5 ppm) and upfield (δ 5.77 ppm, $\Delta\delta$ −0.19 ppm), respectively, compared to those of free EDA and L-**3a** (see: Zingg, S. P.; Arnett, E. M.; McPhail, A. T.; Bothner-By, A. A.; Gilkerson, W. R. *J. Am. Chem. Soc.* **1988**, *110*, 1565−1580). Elemental analysis of the precipitate satisfied the 1:1 stoichiometry.

(37) Direct determination of the de value for (*M*)-**1a**$_3$·(BuCYA)$_6$ was attempted by adding Pirkle reagent. However, the reagent itself acted as chiral auxiliary to induce the chirality in the racemic mixture of (*P*)- and (*M*)-**1a**$_3$·(BuCYA)$_6$.

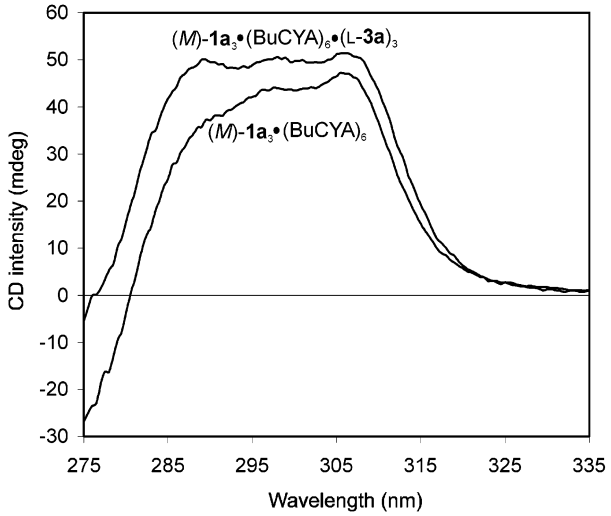

Figure 8. CD spectra of (*M*)-**1a**$_3$·(BuCYA)$_6$·(L-**3a**)$_3$ and (*M*)-**1a**$_3$·(BuCYA)$_6$ in toluene-d_8 at 20 °C. The two assemblies were obtained from the racemic mixture of **1a**$_3$·(BuCYA)$_6$ by treatment with L-**3a** and subsequently with EDA: [**1a**$_3$·(BuCYA)$_6$] = 1 mM, [L-**3a**]/[**1a**$_3$·(BuCYA)$_6$] = 3/1, [EDA]/[L-**3a**] = 1/1 (condition A).

Table 4. Rate Constants (k_{rac}, sec^{-1}) for the Racemization of (*M*)-**1a**$_3$·(BuCYA)$_6$[a]

temp (°C)	condition A[b]	condition B[b]	condition C[b]
80	1.93×10^{-3}	1.92×10^{-3}	4.82×10^{-3}
70	6.30×10^{-4}	6.08×10^{-4}	2.48×10^{-3}
60	1.67×10^{-4}	1.65×10^{-4}	9.22×10^{-4}
60	1.61×10^{-4} [c]		
60	1.67×10^{-4} [d]		
50	4.56×10^{-5}	4.04×10^{-5}	3.42×10^{-4}

[a] Conditions: toluene-d_8, [**1a**$_3$·(BuCYA)$_6$] = 1 mM. [b] Condition A: [L-**3a**]/[**1a**$_3$·(BuCYA)$_6$] = 3/1, [EDA]/[L-**3a**] = 1/1; Condition B: [L-**3a**]/[**1a**$_3$·(BuCYA)$_6$] = 2.1/1, [EDA]/[L-**3a**] = 1/1; Condition C: [L-**3a**]/[**1a**$_3$·(BuCYA)$_6$] = 2.1/1, [EDA]/[L-**3a**] = 2/1. [c] [**1a**$_3$·(BuCYA)$_6$] = 2 mM. [d] [**1a**$_3$·(BuCYA)$_6$] = 0.5 mM.

Racemization of Enantiomeric Assembly. To determine the kinetic stability of (*M*)-**1a**$_3$·(BuCYA)$_6$, the time dependence of CD intensity at 306 nm was monitored under three different conditions: Condition A: [L-**3a**]/[**1a**$_3$·(BuCYA)$_6$] = 3/1, [EDA]/[L-**3a**] = 1/1; Condition B: [L-**3a**]/[**1a**$_3$·(BuCYA)$_6$] = 2.1/1, [EDA]/[L-**3a**] = 1/1; Condition C: [L-**3a**]/[**1a**$_3$·(BuCYA)$_6$] = 2.1/1, [EDA]/[L-**3a**] = 2/1.

Under condition A, the CD intensity at 306 nm hardly decreased after 3 h (only 2−3% reduction), indicating that (*M*)-**1a**$_3$·(BuCYA)$_6$ is kinetically very stable and its racemization is very slow at 20 °C (Figure 9c). At higher temperatures (50, 60, 70, and 80 °C) the kinetic stability decreases (Figure 9c). The time-dependent CD changes follow first-order kinetics (Scheme 2). The rate constants (k_{rac}) for the racemization of (*M*)-**1a**$_3$·(BuCYA)$_6$ were estimated by linear regression analysis (Table 4). The racemization was not dependent on the concentration, supporting the first-order kinetic model (Table 4).

Arrhenius plots of k_{rac} (Figure 10), give the thermodynamic parameters. Under condition A, values for E_a = 119 kJ mol^{-1}, $\Delta G^{\ddagger}_{20}$ = 107 kJ mol^{-1}, $\Delta H^{\ddagger}_{20}$ = 116 kJ mol^{-1}, and $\Delta S^{\ddagger}_{20}$ = 32.8 J mol^{-1} K^{-1} were obtained. The parameters indicate that the induced chirality would be preserved for ca. 1 week at 20 °C and for ca. 1 year at 0 °C (half-life time). Almost the same kinetic stability was observed under condition B (Figure 9b).[38] The observed high kinetic stability of this system (conditions A and B) is attributed to the need to break 12 hydrogen bonds

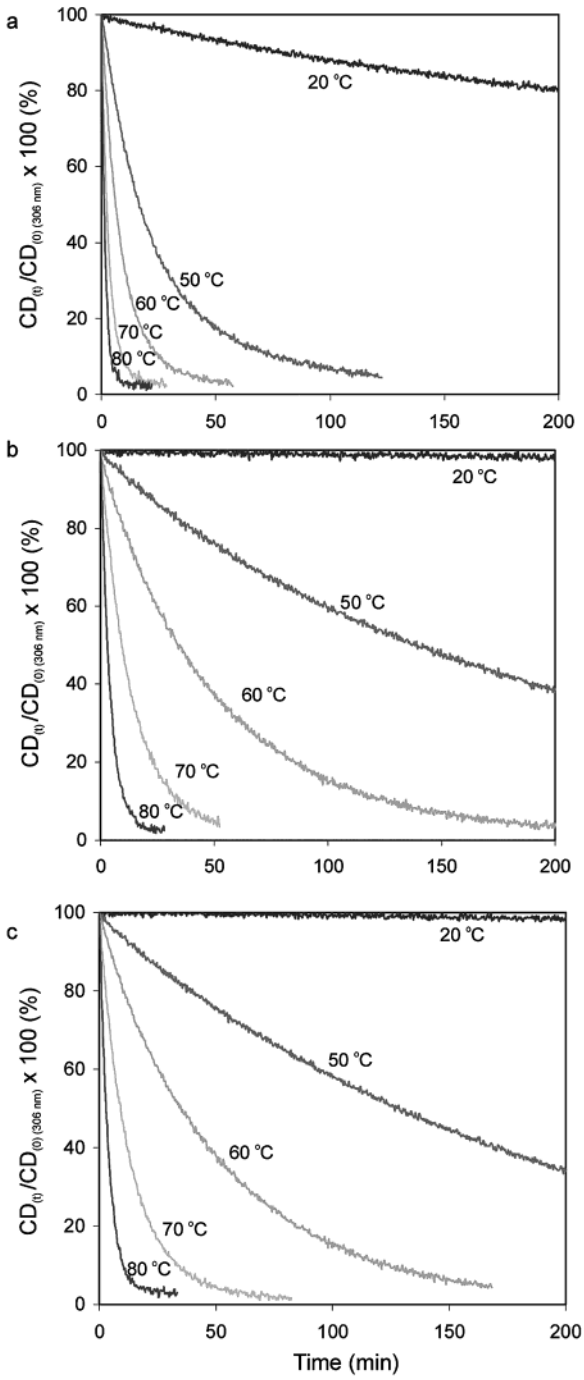

Figure 9. Time dependence of the CD intensity (mdeg) at 306 nm reflecting the racemization of (*M*)-**1a**$_3$·(BuCYA)$_6$ at 20, 50, 60, 70, and 80 °C (in toluene-d_8, [**1a**$_3$·(BuCYA)$_6$] = 1mM): (a) [L-**3a**]/[**1a**$_3$·(BuCYA)$_6$] = 2.1/1, [EDA]/[L-**3a**] = 2/1 (condition C), (b) [L-**3a**]/[**1a**$_3$·(BuCYA)$_6$] = 2.1/1, [EDA]/[L-**3a**] = 1/1 (condition B), (c) [L-**3a**]/[**1a**$_3$·(BuCYA)$_6$] = 3/1, [EDA]/[L-**3a**] = 1/1 (condition A).

for the dissociation of one calix[4]arene-dimelamine moiety from (*M*)-**1a**$_3$·(BuCYA)$_6$, which is the rate-determinating step in the dissociative racemization mechanism (Scheme 3).[24]

Previously, we have reported the formation of an enantiomerically pure double rosette assembly based on a memory

(38) Although under condition A a trace amount of precipitate (diastereomeric assembly) was formed after the addition of L-**3a**, the precipitate redissolved in toluene after the subsequent addition of EDA. Judging from the similar results under conditions A and B (Figure 9c and 9b), there is no need to consider this precipitate.

Scheme 3. Schematic Representation of the Dissoiative Mechanism for Racemization between (*M*)-**1a**$_3$·(BuCYA)$_6$ and (*P*)-**1a**$_3$·(BuCYA)$_6$

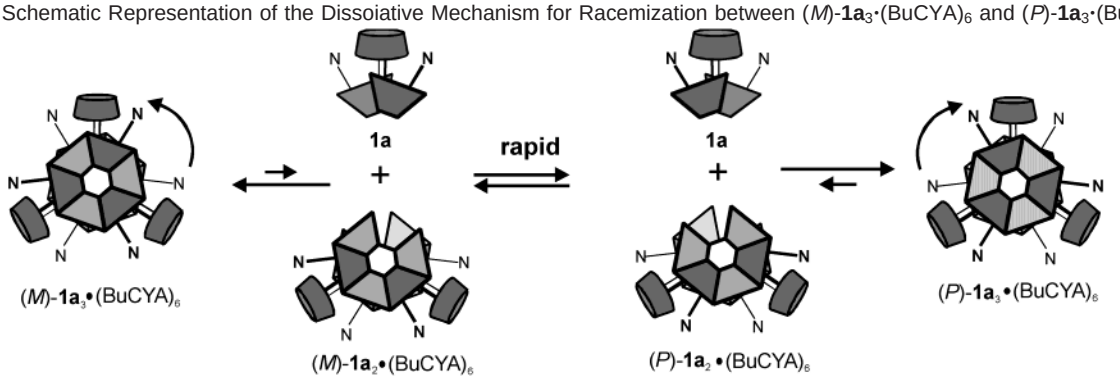

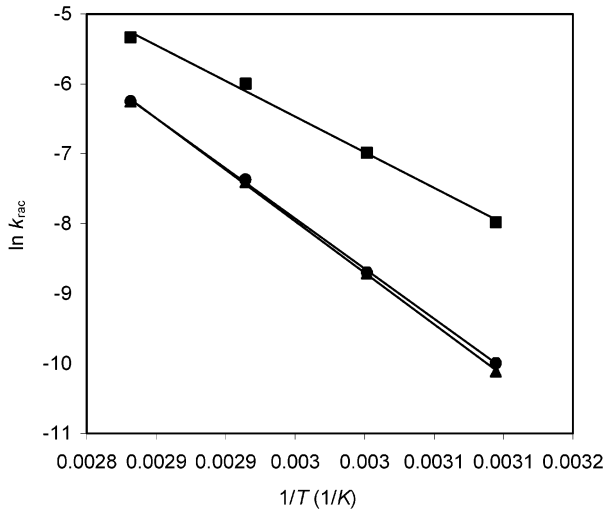

Figure 10. Arrhenius plots for the racemization of (*M*)-**1a**$_3$·(BuCYA)$_6$ under conditions A (●), B (▲), and C (■) (for data and conditions see Table 4).

concept. A chiral barbituric acid (BAR) induces chirality in the assembly, which is preserved after the exchange of BAR to an achiral cyanuric acid. This system has the disadvantage that the racemization of the enantiomerically pure assembly is catalyzed by the liberated BAR.[24] Compared to this system (E_a = 106 kJ mol^{-1} and half-life time of 3 days at 20 °C in benzene-d_6), the present assemblies have a higher kinetic stability (E_a = 119 kJ mol^{-1} and half-life time of 1 week at 20 °C), because the two additives L-**3a** and EDA are completely removed as a precipitate and only (*M*)-**3a**$_3$·(BuCYA)$_6$ is present in solution (conditions A and B).[39]

On the other hand, when we used excess of EDA ([EDA]/[L-**3a**] = 2/1, condition C), the kinetic stability significantly decreased (E_a = 84.8 kJ mol^{-1}, Figures 9a and 10). The half-life time was reduced to only 7 h at 20 °C and 4 days at 0 °C. The lower kinetic stability is attributed to the catalytic role of the excess EDA in accelerating the racemization process. EDA might interact with the acidic cyanuric NH proton of the assembly and dissociate one calix[4]arene-dimelamine moiety.

There is still one point unclear about the present memory system. In chiral complexation of L-**3a** with **1a**$_3$·(BuCYA)$_6$, the chiral induction is achieved via *P*-and *M*-interconversion process as shown in Scheme 4. Compared to the slow racemization of (*M*)-**1a**$_3$·(BuCYA)$_6$ (half-life time, ca. 1 week), the chiral

Scheme 4. Interconversion between (*M*)-**1a**$_3$·(BuCYA)$_6$·(L-**3a**)$_n$ and (*P*)-**1a**$_3$·(BuCYA)$_6$·(L-**3a**)$_n$

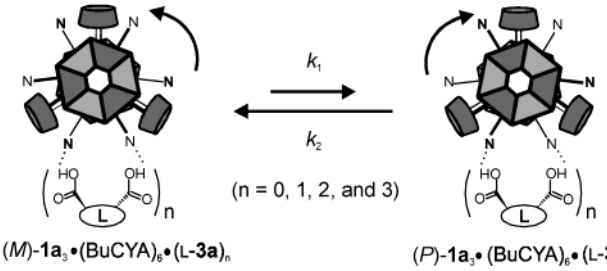

complexation needed only ~15 h to reach equilibrium at 20 °C. To elucidate the rapid interconversion within the system, we monitored the time dependence of CD intensity at 306 nm under two different conditions (Figure 11): Condition X: [L-**3a**]/[**1a**$_3$·(BuCYA)$_6$] = 2.1/1; Condition Y: [L-**3a**]/[**1a**$_3$·(BuCYA)$_6$] = 1/1.

The observed time-dependent CD changes were analyzed according to the model presented in Scheme 4 and the rate constants k_1 (from *M* to *P*) and k_2 (from *P* to *M*) were estimated by linear regression analysis (Table 5). In this model, we used the assumption that in the dynamic equilibrium the two diastereoisomers, (*M*)-**1a**$_3$·(BuCYA)$_6$·(L-**3a**)$_n$ and (*P*)-**1a**$_3$·(BuCYA)$_6$·(L-**3a**)$_n$, could be regarded as averaged mixtures of 1:0, 1:1, 1:2, and 1:3 complexes.[40]

The estimated k_1 and k_2 values change with the amount of L-**3a** (Table 5). At 20 °C, the interconversion rate under condition X (2.1 equiv of L-**3a**) is 5−6 times faster compared to that of the condition Y (1.0 equiv of L-**3a**).[41] The results suggest that the *P*- and *M*-interconversion is catalyzed by L-**3a** similarly to the EDA-catalyzed racemization described above. Thus, the diacid L-**3a** acts as both chiral auxiliary to induce chirality and catalyst to accelerate *P*- and *M*-interconversion. The acid L-**3a** can interact with the basic nitrogen of the melamine in the assembly dissociating one calix[4]arene-dimelamine moiety.

Arrhenius plots of the k_1 and k_2 values (Figure 12) gave activation energies (E_a) of 63.8 (from *M* to *P*) and 45.3 (from *P* to *M*) kJ mol^{-1} under condition X or 92.9 (from *M* to *P*) and 87.5 kJ mol^{-1} (from *P* to *M*) under condition Y. The small E_a

(39) Although the previous memory system has the advantage of (i) exchange in a more apolar solvent (benzene) and (ii) stabilization by the nitro groups attached on calixarene-benzene rings (for detail see ref 15), the present system has a higher kinetic stability.

(40) The *P*- and *M*-interconversion process is slow on the NMR time scale, as indicated by the separated signals corresponding to the *P*- and *M*-isomers. In contrast, the pyridine−carboxylic acid exchange process is quite rapid because we observed only an averaged spectrum of 1:0, 1:1, 1:2, and 1:3 complexes of each *P*- and *M*-isomer.

(41) By increasing the temperature, the trend inverted (Table 5). At 60 °C, a slow interconversion was observed under the condition X (2.1 equiv of L-**3a**), suggesting that at higher temperature the *P*- and *M*-interconversion involves both the catalyzed and uncatalyzed pathways.

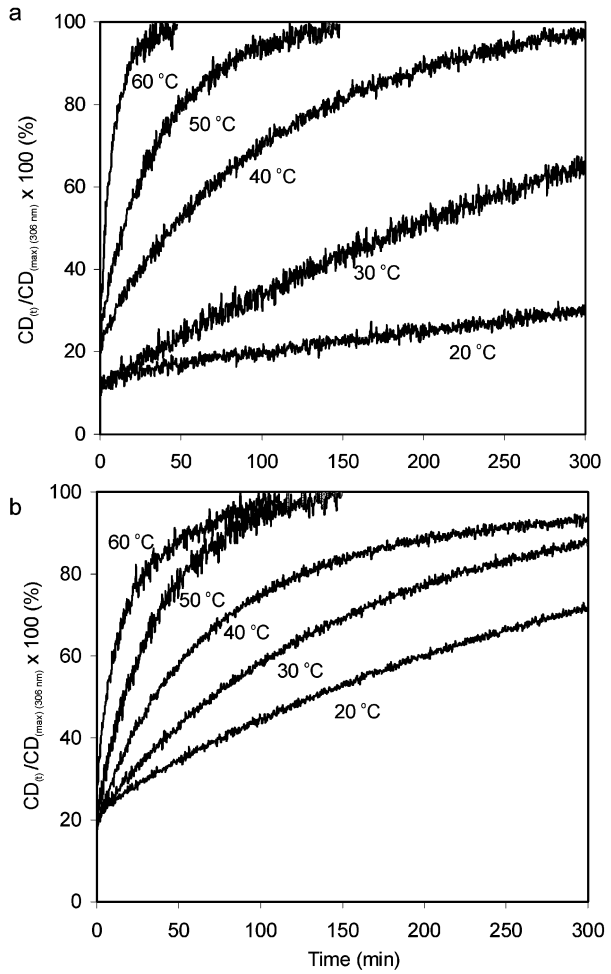

Figure 11. Time dependence of the CD intensity (mdeg) at 306 nm reflecting the interconversion between (*M*)-**1a**$_3$·(BuCYA)$_6$·(L-**3a**)$_n$ and (*P*)-**1a**$_3$·(BuCYA)$_6$·(L-**3a**)$_n$ at 20, 30, 40, 50, and 60 °C: in toluene-d_8, [**1a**$_3$·(BuCYA)$_6$] = 1mM; (a) [L-**3a**]/[**1a**$_3$·(BuCYA)$_6$] = 1.0/1 (condition Y), (b) [L-**3a**]/[**1a**$_3$·(BuCYA)$_6$] = 2.1/1 (condition X).

Table 5. Rate Constants (k_1 and k_2) for the Interconversion between (*M*)-**1a**$_3$·(BuCYA)$_6$·(L-**3a**)$_n$ and (*P*)-**1a**$_3$·(BuCYA)$_6$·(L-**3a**)$_n$[a]

condition[b]	temp (°C)	[*M*]/[*P*][c]	k_1+k_2 (sec^{-1})[d]	k_1 (sec^{-1})[e]	k_2 (sec^{-1})[e]
X	60	71.5/28.5	7.72×10^{-4}	2.20×10^{-4}	5.52×10^{-4}
X	50	75.5/24.5	4.43×10^{-4}	1.06×10^{-4}	3.27×10^{-4}
X	40	80/20	2.04×10^{-4}	4.07×10^{-5}	1.63×10^{-4}
X	30	84.5/15.5	1.05×10^{-4}	1.61×10^{-5}	8.84×10^{-4}
X	20	87/13	5.58×10^{-5}	7.25×10^{-6}	4.85×10^{-5}
Y	60	58/42	1.95×10^{-3}	8.19×10^{-4}	1.13×10^{-3}
Y	50	60/40	4.36×10^{-4}	1.74×10^{-4}	2.61×10^{-4}
Y	40	62/38	1.57×10^{-4}	5.95×10^{-5}	9.70×10^{-5}
Y	30	63.5/36.5	5.15×10^{-5}	1.88×10^{-5}	3.27×10^{-5}
Y	20	65/35	1.23×10^{-5}	4.31×10^{-6}	8.00×10^{-6}

[a] Conditions: toluene-d_8, [**1a**$_3$·(BuCYA)$_6$] = 1 mM. [b] Condition X: [L-**3a**]/[**1a**$_3$·(BuCYA)$_6$] = 2.1/1, Condition Y: [L-**3a**]/[**1a**$_3$·(BuCYA)$_6$] = 1/1. [c] Molar ratio of (*M*)-**1a**$_3$·(BuCYA)$_6$·(L-**3a**)$_n$ and (*P*)-**1a**$_3$·(BuCYA)$_6$·(L-**3a**)$_n$ determined by integration of the ^{1}H NMR signals H^{a1} and H^{a2}. [d] Estimated from the time-dependent CD change (see Figure 11). [e] Estimated from the equation for K = [(*P*)-**1a**$_3$·(BuCYA)$_6$·(L-**3a**)$_n$]/[(*M*)-**1a**$_3$·(BuCYA)$_6$·(L-**3a**)$_n$] = k_1/k_2.

values observed under condition X suggest that the acid-catalyzed *P*- and *M*-interconversion is significantly accelerated, when excess of L-**3a** was used.

Conclusions

In this study, we have demonstrated that addition of an external chiral auxiliary to a racemic mixture of *P*- and *M*-assemblies leads to the formation of mainly one of the two possible diastereomeric assemblies. The enantioselectivity is ascribed to self-selection between *M*-enantiomeric assembly and L-diacid or between *P*-assembly and D-diacid. More interestingly, removal of the chiral auxiliary leaves one of the original enantiomers in 90% ee. This enantiomer is kinetically very stable and racemizes only slowly.

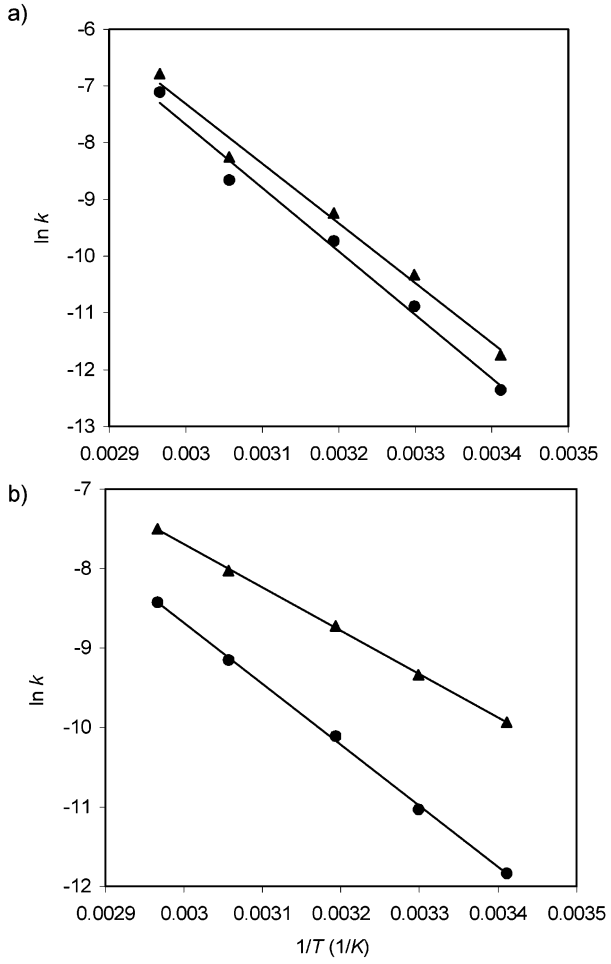

Figure 12. Arrhenius plots for the interconversion between (*M*)-**1a**$_3$·(BuCYA)$_6$·(L-**3a**)$_n$ and (*P*)-**1a**$_3$·(BuCYA)$_6$·(L-**3a**)$_n$: (a) [L-**3a**]/[**1a**$_3$·(BuCYA)$_6$] = 1.0/1 (condition Y) (for data and conditions see Table 5): k_1 (●) and k_2 (▲), (b) [L-**3a**]/[**1a**$_3$·(BuCYA)$_6$] = 2.1/1 (condition X).

Experimental Section

General. All melting points are uncorrected. IR spectra were recorded on a Perkin-Elmer BX spectrophotometer and measured as KBr pellets. ^{1}H NMR spectra were determined in toluene-d_8, DMSO-d_6, or CD_3OD with a Varian Unity 300 spectrometer. Residual solvent protons were used as internal standard and chemical shifts are given relative to tetramethylsilane (TMS). FAB-MS spectra were recorded with a Finnigan MAT 90 spectrometer with *m*-nitrobenzyl alcohol (NBA) as a matrix. CD spectra were measured on a JASCO J-715 spectropolarimeter in a 0.01-cm width cell. Chiral carboxylic acids **2** and **3** are commercially available and were used without purification. Compound **1d** was prepared according to methods described previously.[21]

5,17-*N*,*N*′-Bis{4-amino-6-[(2-pyridyl)methylamino]-1,3,5-triazine-2-yl}diamino-25,26,27,28-tetrakis(propyl)calix[4]arene (1a). A suspension of **1d** (220 mg, 0.25 mmol) in 2-aminomethylpyridine (5 mL) was heated at 90 °C for 16 h under a nitrogen atmosphere. After the

reaction mixture was cooled to room temperature, water (15 mL) and methanol (15 mL) were added. The white precipitate was collected by filtration and washed with water (20 mL). The obtained white solid was dissolved in dichloromethane (3 mL) and methanol (3 mL), and then *n*-hexane (5 mL) was added. The obtained white precipitate was collected by filtration and washed with *n*-hexane (3 mL) to give **1a** in 80% yield (205 mg, 0.2 mmol) as a white solid; mp 275−276 °C; IR (KBr) ν_{max} 3308−3100 (ν_{NH}) cm^{-1}; ^{1}H NMR (DMSO-d_6) δ 0.87, 1.07 (t, J = 7.3 Hz, each 6 H, CH_3), 1.76−1.96 (m, 8 H, CH_2), 2.91, 3.09 (br-d, J = 13.1 Hz, each 2 H, $ArCH_2Ar$), 3.61 (t, J = 6.6 Hz, 4 H, OCH_2), 3.77−3.93 (m, 4 H, OCH_2), 4.17−4.36 (m, 4 H, $ArCH_2Ar$), 4.54−4.65 (m, 4 H, CH_2Py), 6.02−6.38 (m, 10 H, ArH and NH), 7.10−7.50 (m, 10 H, ArH and NH), 7.66−7.78 (m, 2 H, ArH), 8.33−8.66 (m, 4 H, ArH and NH); FAB−MS (positive, NBA) 1023.4 [$(M + H)^+$, calcd 1023.5]. Anal. Calcd for $C_{58}H_{66}N_{14}O_4$: C, 68.08; H, 6.50; N, 19.16. Found: C, 67.78; H, 6.55; N, 19.45.

5,17-*N,N′*-Bis{4-amino-6-[(3-pyridyl)methylamino]-1,3,5-triazine-2-yl}diamino-25,26,27,28-tetrakis(propyl)calix[4]arene (1b). According to a method similar to the preparation of **1a**, **1b** was obtained in 33% yield from **1d** and 3-aminomethylpyridine. The crude product was purified by silica gel column chromatography eluting with dichloromethane/methanol/NH_4OH (95:4.5:0.5, v/v/v) to give **1b** as a white solid: mp 181−183 °C; IR (KBr) ν_{max} 3310−3100 (ν_{NH}) cm^{-1}; ^{1}H NMR (DMSO-d_6) δ 0.87, 1.05 (t, J = 7.3 Hz, each 6 H, CH_3), 1.77−1.97 (m, 8 H, CH_2), 2.85−3.14 (m, 4 H, $ArCH_2Ar$), 3.56−3.66, 3.82−3.93 (m, each 4 H, OCH_2), 4.22−4.38 (m, 4 H, $ArCH_2Ar$), 4.46−4.58 (m, 4 H, CH_2Py), 6.12−6.40 (m, 10 H, ArH and NH), 7.22−7.49 (m, 8 H, ArH and NH), 7.63−7.77 (m, 2 H, ArH), 8.35−8.69 (m, 6 H, ArH and NH); FAB−MS (positive, NBA) 1023.5 [$(M + H)^+$, calcd 1023.5]. Anal. Calcd for $C_{58}H_{66}N_{14}O_4$: C, 68.08; H, 6.50; N, 19.16. Found: C, 67.84; H, 6.30; N, 19.06.

5,17-*N,N′*-Bis{4-amino-6-[(4-pyridyl)methylamino]-1,3,5-triazine-2-yl}diamino-25,26,27,28-tetrakis(propyl)calix[4]arene (1c). According to a method similar to the preparation of **1a**, **1c** was obtained in 50% yield from **1d** and 4-aminomethylpyridine. The crude product was purified by silica gel column chromatography eluting with dichloromethane/methanol/NH_4OH (95:4.5:0.5, v/v/v) to give **1c** as a white solid: mp 178−180 °C; IR (KBr) ν_{max} 3310−3100 (ν_{NH}) cm^{-1}; ^{1}H NMR (DMSO-d_6) δ 0.87 (t, J = 6.6 Hz, 6 H, CH_3), 1.07 (t, J = 7.3 Hz, 6 H, CH_3), 1.75−1.96 (m, 8 H, CH_2), 2.76−2.96, 3.02−3.14 (m, each 2 H, $ArCH_2Ar$), 3.53−3.66, 3.79−3.92 (m, each 4 H, OCH_2), 4.17−4.37 (m, 4 H, $ArCH_2Ar$), 4.47−4.57 (m, 4 H, CH_2Py), 6.03−6.38 (m, 10 H, ArH and NH), 7.20−7.50 (m, 10 H, ArH and NH), 8.36−8.70 (m, 6 H, ArH and NH); FAB−MS (positive, NBA) 1024.1 [$(M + H)^+$, calcd 1023.5]. Anal. Calcd for $C_{58}H_{66}N_{14}O_4$: C, 68.08; H, 6.50; N, 19.16. Found: C, 68.25; H, 6.45; N, 18.43.

General Procedure for the Preparation of Rosette Assemblies 1a−c$_3$·(BuCYA)$_6$. 3 Equivalents of **1a−c** and 6 equiv of BuCYA were mixed in toluene-d_8 (at 1 mM for the rosette assembly). The mixtures were heated until the solids were dissolved and then equilibrated for 15 h. ^{1}H NMR data are assigned to one unit of **1a−c**.

For **1a**$_3$·(BuCYA)$_6$ (D_3 = 100%): ^{1}H NMR (toluene-d_8) δ 0.87 (t, J = 7.1 Hz, 6 H, CH_3), 1.03 (t, J = 7.5 Hz, 12 H, CH_3), 1.40−2.05 (m, 16 H, CH_2), 3.21, 3.29, 4.61, 4.62 (d, J = 13.6 Hz, each 2 H, $ArCH_2Ar$), 3.54 (t, J = 6.6 Hz, 4 H, OCH_2), 4.04−4.37 (m, 8 H, OCH_2 and NCH_2), 4.71 (dd, J = 4.0, 15.9 Hz, 2 H, CH_2Py), 5.64 (dd, J = 7.9, 15.9 Hz, 2 H, CH_2Py), 6.36 (d, J = 2.2 Hz, 2 H, Hh), 6.71 (t, J = 7.5 Hz, 2 H, H5−Py), 7.12 (dt, J = 1.8, 7.5 Hz, 2 H, H4−Py), 7.27 (t, J = 7.1 Hz, 2 H, ArH), 7.37 (d, J = 7.1 Hz, 2 H, ArH), 7.50 (d, J = 7.5 Hz, 2 H, H3−Py), 7.73−7.78 (m, 4 H, Hg and ArH), 7.82 (s, 2 H, NHe), 8.06 (s, 2 H, NHf), 8.59 (dd, J = 1.8, 7.5 Hz, 2 H, H6−Py), 8.69 (dd, J = 4.0, 7.9 Hz, 2 H, NHd), 9.18 (s, 2 H, NHc), 14.49 (s, 2 H, NHb), 14.95 (s, 2 H, NHa).

For **1b**$_3$·(BuCYA)$_6$ (D_3:C_{3h}:C_s = 78:10:12): ^{1}H NMR (toluene-d_8) for D_3-isomer δ 0.86, 1.04, 1.15 (t, J = 7.5 Hz, each 6 H, CH_3), 1.47−2.14 (m, 16 H, CH_2), 3.21 (d, J = 13.7 Hz, 2 H, $ArCH_2Ar$), 3.51−3.64 (m, 6 H, $ArCH_2Ar$ and OCH_2), 4.03−4.34 (m, 8 H, OCH_2 and NCH_2), 4.54−4.70 (m, 6 H, $ArCH_2Ar$ and CH_2Py), 5.30 (dd, J = 7.9, 14.6 Hz, 2 H, CH_2Py), 6.36 (d, J = 2.2 Hz, 2 H, Hh), 6.78−8.00 (m, 16 H, ArH and NH), 8.46−8.60 (m, 4 H, NHd and H6−Py), 9.09 (d, J = 2.2 Hz, 2 H, H2−Py), 9.13 (s, 2 H, NHc), 14.40 (s, 2 H, NHb), 14.79 (s, 2 H, NHa); for C_{3h}-isomer 14.63 (s, 2 H, NHb), 15.04 (s, 2H, NHa); for C_s-isomer 14.33 (s, 1 H for assembly, Hb), 14.75−14.83 (m, 3 H for assembly, Ha and Hb), 15.19, 15.22 (s, each 1H for assembly, Ha).

For **1c**$_3$·(BuCYA)$_6$ (D_3:C_{3h}:C_s = 20:20:60): ^{1}H NMR (toluene-d_8) δ 14.44 (s, C_{3h}-NHb), 14.68 (s, D_3-NHb), 14.74 (s, C_s-NHb), 14.79 (s, C_{3h}-NHa or C_s-NHb), 14.83(s, C_{3h}-NHa or C_s-NHb), 14.85 (s, C_s-NHb), 15.07 (s, D_3-NHa), 15.15 (s, C_s-NHa), 15.17 (s, C_s-NHa), 15.19 (s, C_s-NHa). Because of the overlap of the spectra for the three isomers, only the lower magnetic field region was assigned.

EDA·L-3a 1:1 Complex. To a stock solution (2 mL, 1 mM of assembly) of **1a**$_3$·(BuCYA)$_6$·(L-**3a**)$_3$, which was prepared from **1a** (15.4 mg, 0.015 mmol), BuCYA (5.6 mg, 0.03 mmol), and L-**3a** (5.4 mg, 0.015 mmol, COOH/pyridine = 1/1) in toluene-d_8 (5 mL), was added 15 mM toluene solution of EDA (40 μL, 0.006 mmol, NH_2/COOH = 1/1) at 0 °C. The white precipitate was collected by filtration and washed with toluene (2 mL) to quantitatively give EDA·L-**3a**: ^{1}H NMR (CD_3-OD) δ 3.17 (s, 4 H, CH_2N), 5.77 (s, 2 H, CHCOO), 7.46 (t, J = 7.3 Hz, 4 H, *m*-ArH), 7.59 (t, J = 7.3 Hz, 2 H, *p*-ArH), 8.14 (d, J = 7.3 Hz, 4 H, *o*-ArH); Anal. Calcd for $C_{20}H_{22}N_2O_8$: C, 57.41; H, 5.30; N, 6.70. Found: C, 57.14; H, 5.34; N, 6.68.

General Procedure for the Monitoring Racemization of (M)-1a$_3$·(BuCYA)$_6$. To a stock solution (2 mL, 1 mM of assembly) of (*M*)-**1a**$_3$·(BuCYA)$_6$·(L-**3a**)$_3$, which was prepared from **1a** (15.4 mg, 0.015 mmol), BuCYA (5.6 mg, 0.03 mmol), and L-**3a** (5.4 mg, 0.015 mmol, COOH/pyridine = 1/1) in toluene-d_8 (5 mL), was added 15 mM toluene solution of EDA (40 μL, 0.006 mmol, NH_2/COOH = 1/1) at 0 °C. A white precipitate of 1:1 complex EDA·L-**3a** was immediately formed. The supernatant solution was subjected to a CD cell heated at measurement temperature, and the CD measurement was started immediately.

The observed time-dependent CD changes satisfied first-order kinetics (Scheme 2), in which k_{rac} (sec^{-1}) is the rate constant for the racemization. Linear regression analysis of the CD data gave the rate constants (k_{rac}). Half-life time ($t_{1/2}$) was obtained from eq 2:

$$t_{1/2} = \ln 2/2k_{rac} = 0.693/2k_{rac} \quad (2)$$

The obtained k_{rac} values were analyzed according to the Arrhenius eq 3:

$$\ln k = \ln A - E_a/RT \quad (3)$$

in which A (sec^{-1}) is the preexponential factor, E_a (kJ mol^{-1}) is the activation energy, R (8.314×10^{-3} kJ K^{-1} mol^{-1}) is the gas constant, and T (K) is the absolute temperature.

General Procedure for the Monitoring Interconversion between (M)-1a$_3$·(BuCYA)$_6$·(L-3a)$_n$ and (P)-1a$_3$·(BuCYA)$_6$·(L-3a)$_n$. A stock solution (1 mL, 1 mM of assembly) of **1a**$_3$·(BuCYA)$_6$·(L-**3a**)$_n$, which was prepared from **1a** (15.4 mg, 0.015 mmol), BuCYA (5.6 mg, 0.03 mmol), and L-**3a** (3.8 mg, 0.0105 mmol, L-**3a**/assembly = 2.1/1) in toluene-d_8 (5 mL), was heated at reflux temperature in a sealed tube and immediately cooled at liquid-nitrogen temperature. The sample was warmed to room temperature and immediately subjected to a CD cell heated at the measurement temperature, and the CD measurement was started immediately.

The observed time-dependent CD changes satisfied a kinetic model of Scheme 4, in which k_1 (from *M* to *P*) and k_2 (from *P* to *M*) (sec^{-1}) are the rate constants for the interconversion of *P* and *M* diastereoisomers. Linear regression analysis of the CD data gave the total rate constants ($k_1 + k_2$). Each value of k_1 and k_2 was estimated from an eq 4:

$$K = [(P)\text{-}\mathbf{1a}_3\cdot(\mathrm{BuCYA})_6\cdot(\text{L-}\mathbf{3a})_n]/[(M)\text{-}\mathbf{1a}_3\cdot(\mathrm{BuCYA})_6\cdot(\text{L-}\mathbf{3a})_n] = k_1/k_2 \quad (4)$$

in which association constant (K) was estimated from the ^{1}H NMR integration ratio of the two diastereomeric assemblies. The obtained k_1 and k_2 values were analyzed according to the Arrhenius eq 3.

Supporting Information Available: Plot of the *de* versus CD, Hill plots, and Scatchard plots for $\mathbf{1a}_3\cdot(\mathrm{BuCYA})_6$ in the presence of L-**3a** and L-**3b**. This material is available free of charge via the Internet at http://pubs.acs.org.

JA0207302